(12)

DNA-TR-83-06

AD A131489

SIMULATION OF A NUCLEAR BLAST WAVE WITH A GASEOUS DETONATION TUBE

R&D Associates
P.O. Box 9693
Marina del Rey, California 90291

1 March 1983

Technical Report

CONTRACT No DNA 001-83-C-0001

APPROVED FOR PUBLIC RELEASE;
DISTRIBUTION UNLIMITED.

THIS WORK WAS SPONSORED BY THE DEFENSE NUCLEAR AGENCY UNDER RDT&E RMSS CODE B310083466 P99QAXMK00038 H2590D.

DTIC FILE COPY

Prepared for
Director
DEFENSE NUCLEAR AGENCY
Washington, DC 20305

83 08 17 027

REPORT DOCUMENTATION PAGE

READ INSTRUCTIONS BEFORE COMPLETING FORM

1. REPORT NUMBER DNA-TR-83-06	2. GOVT ACCESSION NO. AD-A131489	3. RECIPIENT'S CATALOG NUMBER
4. TITLE (and Subtitle) SIMULATION OF A NUCLEAR BLAST WAVE WITH A GASEOUS DETONATION TUBE		5. TYPE OF REPORT & PERIOD COVERED Technical Report
		6. PERFORMING ORG. REPORT NUMBER RDA-TR-125004-003
7. AUTHOR(s) Allen L. Kuhl		8. CONTRACT OR GRANT NUMBER(s) DNA 001-83-C-0001
9. PERFORMING ORGANIZATION NAME AND ADDRESS R & D Associates P. O. Box 9695 Marina del Rey, CA 90291		10. PROGRAM ELEMENT, PROJECT, TASK AREA & WORK UNIT NUMBERS Task P99QAXMK-00038
11. CONTROLLING OFFICE NAME AND ADDRESS Director Defense Nuclear Agency Washington, DC 20305		12. REPORT DATE 1 March 1983
		13. NUMBER OF PAGES 34
14. MONITORING AGENCY NAME & ADDRESS (if different from Controlling Office)		15. SECURITY CLASS. (of this report) UNCLASSIFIED
		15a. DECLASSIFICATION DOWNGRADING SCHEDULE N/A since UNCLASSIFIED

16. DISTRIBUTION STATEMENT (of this Report)

Approved for public release; distribution unlimited.

17. DISTRIBUTION STATEMENT (of the abstract entered in Block 20, if different from Report)

18. SUPPLEMENTARY NOTES

This work was sponsored by the Defense Nuclear Agency under RDT&E RMSS Code B310083466 P99QAXMK00038 H2590D.

19. KEY WORDS (Continue on reverse side if necessary and identify by block number)

Nuclear surface burst
Chapman-Jouguet detonation
Similarity solution
Dusty boundary layer
Static pressure waveforms
Dynamic pressure waveforms
Simulation fidelity

20. ABSTRACT (Continue on reverse side if necessary and identify by block number)

There is an ongoing interest in simulating nonideal blast environments for nuclear effects research. In particular, one would like to be able to impose peaked blast waves on real ground surfaces and experimentally measure the ensuing dusty airblast environment. Proposed here is a gaseous detonation tube blast simulator. A disposable (or reusable) shock tube would be constructed on an in-situ ground surface of interest. The tube would be sealed and filled with a detonatable gas mixture. When a planar detonation

20. ABSTRACT (Continued)
wave is initiated at one end of the tube, it induces a peaked blast wave which expands self-similarly with time--the longer the detonation run distance, the longer the blast wave duration. Similarity analysis of such a wave (which consists of a constant-velocity Chapman-Jouguet detonation followed by an adiabatic rarefaction wave expressed in terms of a Riemann characteristic) results in a closed-form analytic solution for the flow field time history. It is shown that the static and dynamic pressure wave-forms associated with this detonation give a high fidelity simulation of a nuclear surface burst. One can achieve peak overpressures from 14 to 55 atm and peak dynamic pressures from 6 to 35 atm, depending on the detonatable gas selected. Detonation run lengths from 25 to 100 $m/KT_{SB}^{1/3}$ are required for kiloton-level simulations. The principal simulation deficiency involves the detonation temperature (∿3000K) which is considerably larger than its airblast counterpart (∿1000K). Small dust particles have the potential for melting and/or vaporizing, due to convective heat transfer from the detonation products, while in the nuclear case such effects are caused by radiative heating from the fireball. These effects can be ameliorated somewhat by choosing air as the oxidizer, and by employing large diameter dust particles.

TABLE OF CONTENTS

LIST OF ILLUSTRATIONS

1. INTRODUCTION

There is an ongoing interest in simulating nonideal nuclear blast environments for weapons effects research. Gilette et al. (1982) have used a portable wind tunnel to measure the steady flow erosion characteristics of desert soils. We would like to do similar tests with peaked blast waves imposed on real ground surfaces to diagnose experimentally the dusty airblast environment. Dynamic similitude arguments applied to such dusty flows lead to the requirement for large explosive yields.

Solid explosive charges have been used to create surface burst (and more recently, height-of-burst) blast environments for yields as large as a kiloton nuclear equivalent. Such tests are expensive, infrequent, and at present, they give a high-fidelity simulation for peak pressures only below about 80 psi. Large shock-tube facilities (such as Sandia's thunderpipe and the DASACON conical tube) are usually limited to peak pressures of tens of psi, and must necessarily use disturbed soil samples. The dynamic airblast simulator (DABS) concept could be used for creating kiloton-level blast environments (Renick, 1979) with peak pressures of as high as 600 psi, but test times are short (due to the solid explosives combustion products) and such tests have been too expensive for parametric studies. Hence, it appears that the existing blast simulators all have certain limitations for this application. There is a need for a simulator which is capable of producing high-fidelity nuclear blast environments with peak pressures of hundreds of psi and kiloton-level yields on in-situ ground surfaces. Tests run with such a simulator should be inexpensive enough that parametric studies can be performed.

A new concept which may fulfill such requirements is the gaseous detonation tube blast simulator shown in Figure 1. A reusable or disposable shock tube would be constructed over an in-situ ground surface of interest. The tube could, for example, be constructed of concrete sewer pipe of a semi-circular cross section, with a soil overburden to contain the blast. The tube would be sealed and filled with a detonatable gas mixture. The firing of the detonator on the end wall would initiate a detonation wave which would propagate down the tube at a constant velocity, known as the Chapman-Jouguet (CJ) velocity.

The detonation wave induces a peaked blast wave flow field. Figure 2 presents the flow field space distribution of a planar, constant velocity CJ wave. Pressures (p), densities (ρ), internal energies (e) and velocities (u) have been nondimensionalized by their values just behind the detonation wave (denoted by subscript n), while distances are nondimensionalized by the detonation front location. Such a wave expands self-similarly; that is, along lines of r/t = constant the flow field properties remain constant. Also shown in Figure 2 is the flow field corresponding to a point explosion (PE). The pressure and velocity fields for the CJ and PE solutions are qualitatively similar, while the density and internal energy distributions are somewhat different due to the high-temperature fireball in the PE case.

The remainder of the paper investigates the feasibility and characteristics of such a simulator. Section II describes the similarity analysis for one-dimensional CJ detonation waves, and gives a closed-form analytic expression for the planar case. Time histories for the planar CJ solution are then compared and matched in Section III to a 1-KT nuclear surface burst over an ideal surface. Conclusions and recommendations are offered in Section IV.

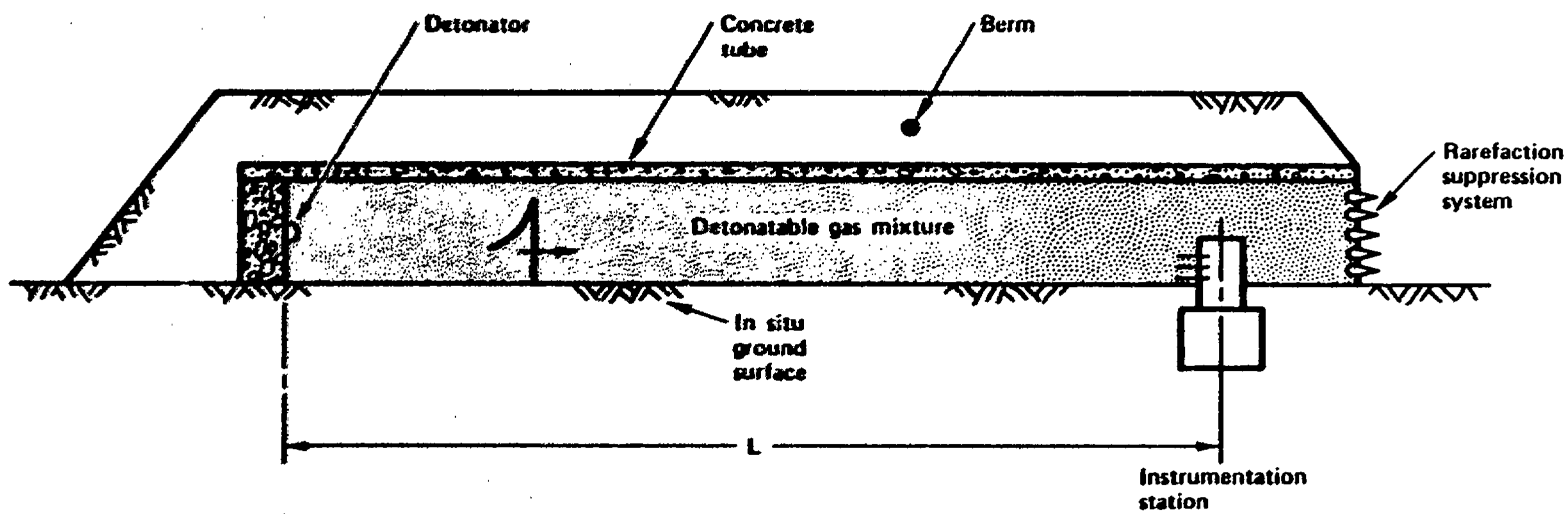

Figure 1. Detonation tube airblast simulator.

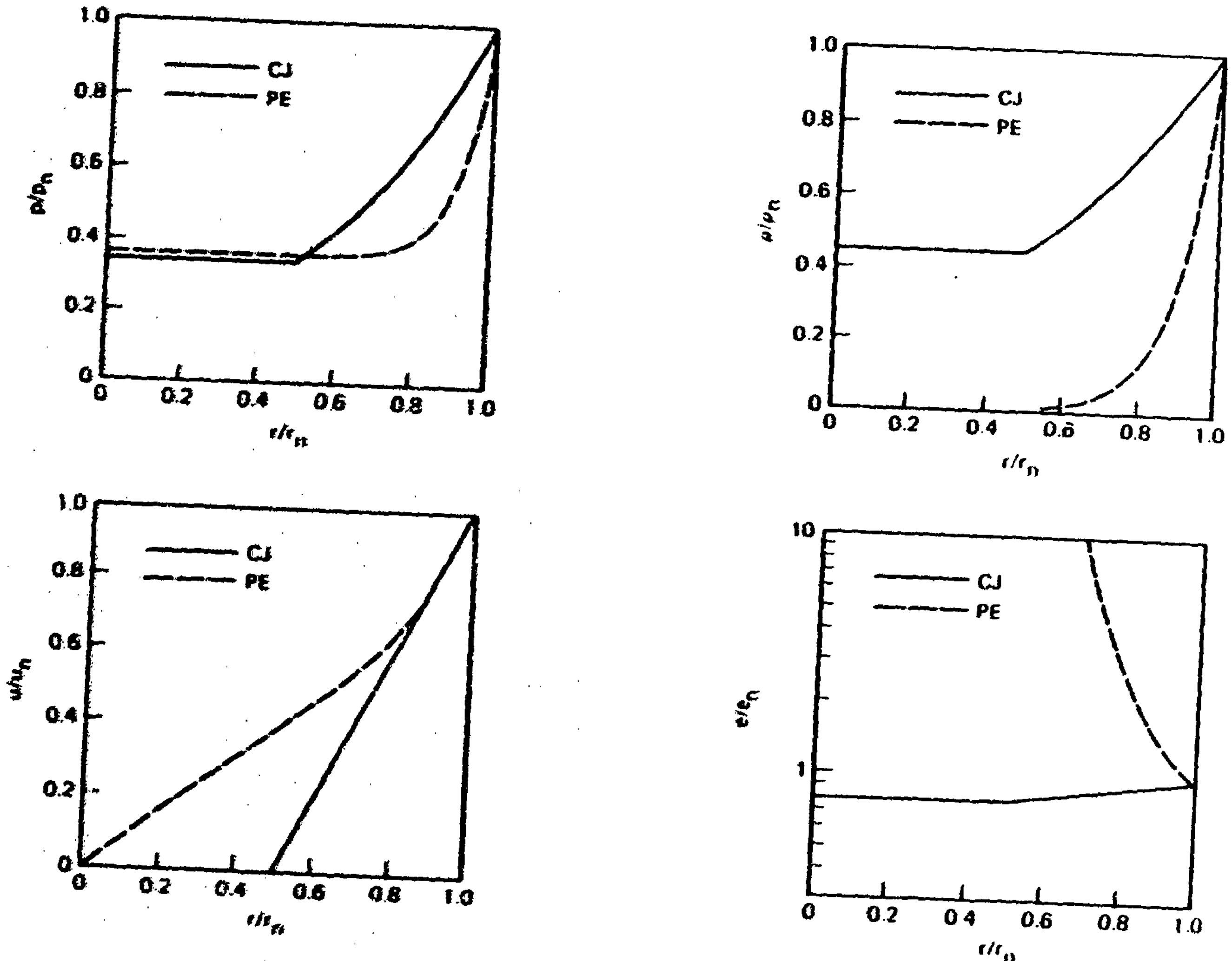

Figure 2. Comparison of the flow fields for a planar Chapman-Jouguet detonation wave (CJ: $j = 0$, $\gamma = 1.3$, $y = 0$) and a spherical point explosion (PE: $j = 2$, $\gamma = 1.4$, $y = 0.10$).

II. SIMILARITY ANALYSIS

1. GOVERNING EQUATIONS

Detonation waves are nonsteady gas dynamic flow fields bounded by shock waves that release chemical energy. Among the first to investigate the properties of such waves were Chapman (1899) and Jouguet (1905-6) who found experimentally that detonation waves propagate at a constant speed. The fundamental theory of detonation waves may be found in the books by Courant and Friedrichs (1948), Stanyukovich (1959), Zeldovich and Kompaneets (1960), and in the treatise by Taylor and Tankin (1958). Analysis of TNT explosions is contained in the work of Taylor (1950). Kuhl and Seizew (1978) compared the flow field of self-similar, planar, cylindrical and spherical detonations in solid and gaseous explosives for the constant velocity case, while Oppenheim et al. (1972) parametrically studied all possible self-similar blast waves bounded by a strong CJ detonation front.

Here we analyze flow fields associated with planar detonations under the following idealized conditions:

- The ambient medium ahead of the wave is quiescent, uniform, and unbounded.
- The detonation propagates at constant velocity.
- The flow field behind the front is adiabatic (no afterburning) with a constant isentropic sound speed modulus.
- The reaction zone is negligibly thin.
- The detonation initiation distance is negligibly small compared to the front radius.
- The flow field is plane symmetrical and unsupported (e.g., by a piston).

As established both theoretically and experimentally, such detonation waves propagate at a constant velocity (the CJ velocity), and satisfy the CJ hypothesis (the wave velocity equals the gas velocity plus the sound speed). The front trajectory is given by

$$r_n = w_n t_n . \tag{1}$$

The flow field behind such a detonation wave is constant along lines of r/t = constant. One can then define similarity variables

$$x = r/r_n \text{ or } \tau = t/t_n \tag{2}$$

and the flow expands self-similarly, i.e., it is constant along lines of x = constant or τ = constant. The analysis of self-similar blast wave flow fields is performed most easily for the so-called phase plane variables:

$$F = u/xw_n = \tau u/w_n \tag{3}$$

$$Z = (a/xw_n)^2 = (\tau a/w_n)^2 \tag{4}$$

where a denotes the isentropic sound speed, $a = \sqrt{\gamma p/\rho}$. For the above assumptions, the conservation laws reduce to a single ordinary differential equation (Kuhl and Seizew, 1978):

$$\frac{dZ}{dF} = \frac{Z}{F}\,\frac{2\underline{D}+j(\gamma-1)(1-F)F}{\underline{D}+jZ} \tag{5}$$

$$\underline{D} = Z-(1-F)^2 \tag{6}$$

and a quadrature

$$\ell n x = -\ell n \tau = -\int \frac{D}{F(D+jZ)}\, dF. \tag{7}$$

The thermodynamic behavior of the medium is characterized by the specific heat ratio, γ, which is assumed to be constant. Flow geometry is taken into account by the paramter j which equals 0, 1 or 2 for plane, line or point symmetric flow.

Equations (5) and (7) are integrated from the wave front (F_n, Z_n, $x = \tau = 1$) to the center of the wave. Given the integral curve $Z = Z(F)$ and $x = x(F)$ (or $\tau = \tau(F)$), the flow field is determined from

$$\begin{aligned} u/u_n &= xF/F_n \\ &= F/\tau F_n \end{aligned} \tag{8}$$

$$e/e_n = (p/p_n)^{(\gamma-1)/\gamma} = (\rho/\rho_n)^{\gamma-1} = x^2 Z/Z_n = Z/\tau^2 Z_n \tag{9}$$

the latter being a consequence of the fact that the flow field behind the detonation wave is homentropic.

2. BOUNDARY CONDITIONS

The physical variables just behind the detonation front are determined from conservation of mass, momentum and energy across the front:

$$\left.\begin{aligned} \rho_n &= \rho_a/(1-F_n) \\ p_n &= p_a + \rho_a F_n w_n^2 \\ e_n &= e_a + \dot{q} + 0.5F_n^2 w_n^2 \\ u_n &= F_n w_n \end{aligned}\right\} \tag{10}$$

written here in terms of F_n, and the chemical energy release, $\dot{q}$. The CJ state, where the wave velocity equals the speed of the characteristic

$$w_n = u_n \pm a_n = w_n \left(F_n \pm \sqrt{Z_n}\right) , \quad (11)$$

then becomes

$$Z_n = (1-F_n)^2$$
$$F_n = (1-y)/(\gamma+1) \quad (12)$$

where y is the front Mach number parameter $y = a_a^2/w_n^2$. Typical detonation Mach numbers are on the order of $M = 5$ ($y \approx 0.04$); hence, the strong shock boundary conditions ($y = 0$) are a good approximation for most problems. The phase plane variables at the detonation front are then

$$F_n = 1/(\gamma+1)$$
$$Z_n = [\gamma/(\gamma+1)]^2 , \quad (13)$$

while the jump conditions reduce to

$$\left.\begin{aligned} \rho_n &= \rho_a(\gamma+1)/\gamma \\ p_n &= p_a+\rho_a w_n^2/(\gamma+1) \\ e_n &= \frac{1}{\gamma-1}\frac{p_n}{\rho_n} \end{aligned}\right\} \quad (14)$$

$$u_n = w_n/(\gamma+1)$$

$$\dot{q} = w_n^2 / 2(\gamma^2-1) \quad . \qquad (14)$$

As shown above, all properties behind strong CJ detonations as well as the heat release at the front are functions of the detonation velocity w_n and γ.

3. PLANAR DETONATIONS

Planar detonations ($j = 0$) represent a singular case in which the solution may be written in closed form. The rarefaction wave behind the detonation front is a centered, simple wave which decelerates the flow to zero velocity ($u = 0$ at $r = 0$). One finds from characteristics theory that along lines of

$$\frac{dr}{dt} = w = u+a$$

$$= xw_n[F+Z^{1/2}] , \qquad (15)$$

the Riemann variable

$$R = u+2a/(\gamma-1)$$

$$= xw_n[F-2Z^{1/2}/(\gamma-1)] \qquad (16)$$

remains constant. Equation (15) can be solved (using the fact that $w = xw_n$) to obtain the integral curve in the phase plane in closed form:

$$Z = (1-F)^2. \qquad (17)$$

Eliminating Z from Equation (16) by virtue of Equation (17), one finds

$$R = xw_n[(\gamma+1)F-2]/(\gamma-1). \qquad (18)$$

Evaluating the Riemann constant of Equation (18) at the detonation front, yields

$$xw_n[(\gamma+1)F-2]/(\gamma-1) = w_n[(\gamma+1)F_n-2]/(\gamma-1); \qquad (19)$$

and solving for x one finds

$$x = \frac{2-(\gamma+1)F_n}{2-(\gamma+1)F}; \qquad (20)$$

or, by virtue of Equation (7), τ becomes:

$$\tau = 1/x = \frac{2-(\gamma+1)F}{2-(\gamma+1)F_n}. \qquad (21)$$

These represent an analytic, closed-form relation for the integral of Equation (7). For the strong shock boundary condition $[(F_n = 1/(\gamma+1))]$, Equation (21) acquires the particularly simple form:

$$\tau = 2-F(\gamma+1). \qquad (22)$$

Equations (17) and (22) can be used to express the phase plane variables in terms of τ:

$$F = (2-\tau)/(\gamma+1) \qquad (23)$$

$$Z = (\gamma+\tau-1)^2/(\gamma+1)^2. \qquad (24)$$

The above relations combined with the boundary conditions [Equations (13) and (14)] can be used in Equations (8) and (9) to give an analytic expression for the flow field of a strong planar CJ detonation wave:

$$u/u_n = 2/\tau-1 \tag{25}$$

$$e/e_n = [(\gamma+\tau-1)/\gamma\tau]^2 \tag{26}$$

$$p/p_n = [(\gamma+\tau-1)/\gamma\tau]^{2\gamma/(\gamma-1)} \tag{27}$$

$$\rho/\rho_n = [(\gamma+\tau-1)/\gamma\tau]^{2/(\gamma-1)} \tag{28}$$

$$q/q_n = (2/\tau-1)^2[(\gamma+\tau-1)/\gamma\tau]^{2/(\gamma-1)} \tag{29}$$

This solution is valid from the head to the tail of the rarefaction wave: $1 \leq \tau \leq 2$. For times greater than $t = 2$, the flow field is constant:

$$u/u_n = 0 \tag{30}$$

$$e/e_n = (\gamma+1)^2/4\gamma^2 \tag{31}$$

The above restrictions allow the solution to satisfy the $u = 0$ condition at the center of symmetry, $x = 0$.

Figure 3 shows the derived similarity solution for a constant-velocity CJ detonation wave ($j = 0$, $y = 0$, $\gamma = 1.3$) as a function of time τ, with all quantities being nondimensionalized by their values at the detonation front. An auxiliary x scale is included to display the space distribution aspects of the flow field. Figure 4 gives the

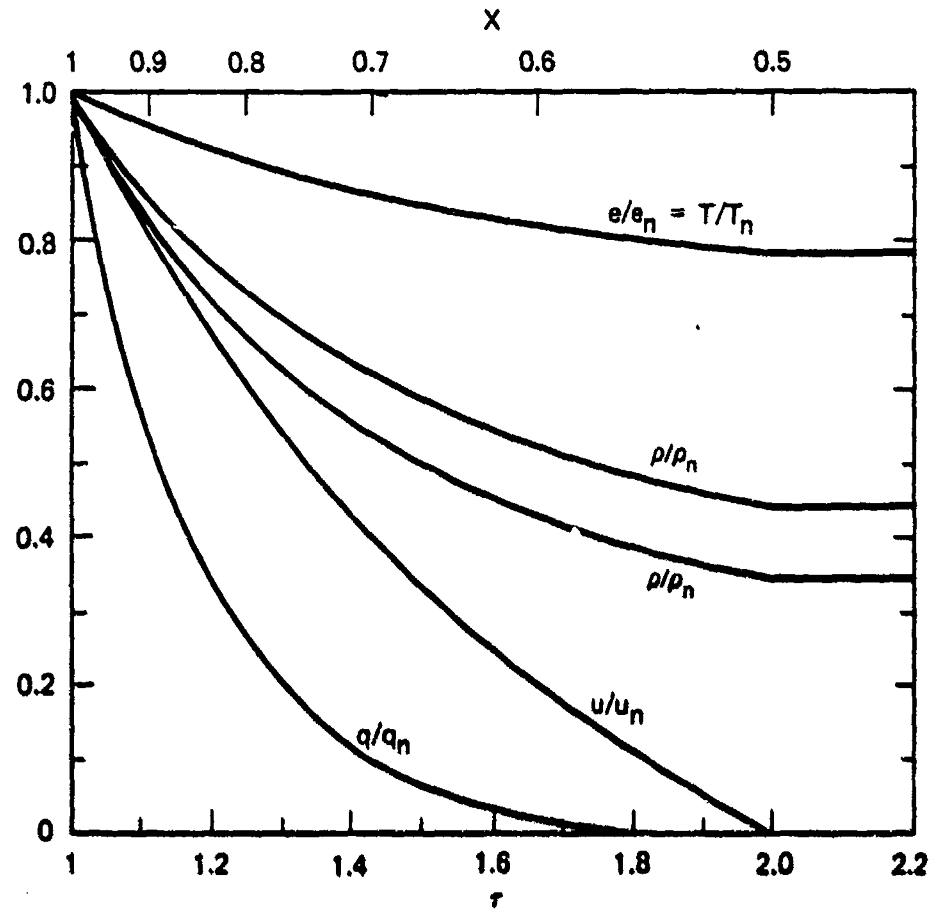

Figure 3. Flow field time history for a planar Chapman-Jouguet detonation wave ($j = 0$, $\gamma = 1.3$, $y = 0$).

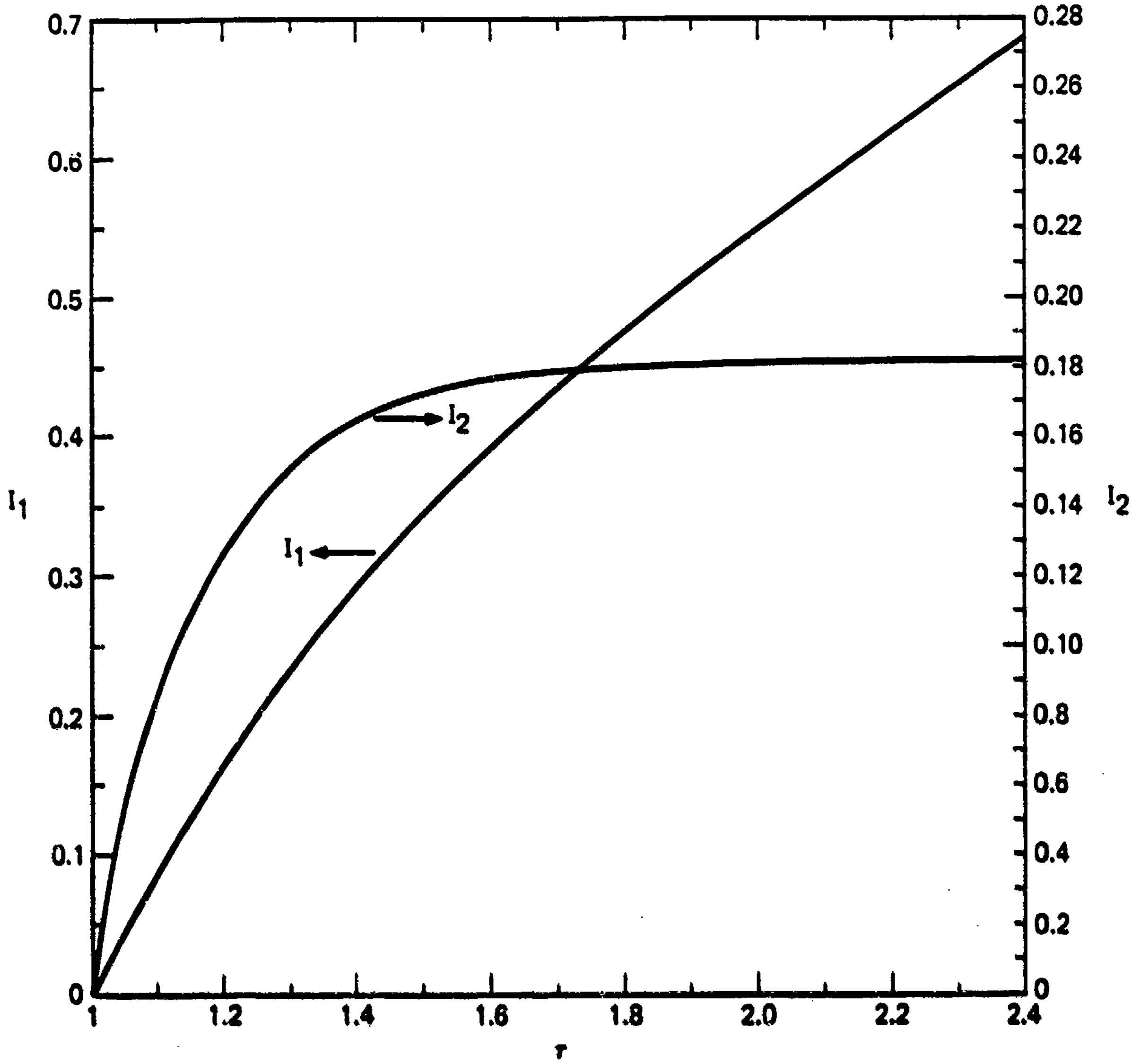

Figure 4. Nondimensional static pressure impulse I_1 and dynamic pressure impulse I_2 vs time for a planar detonation wave ($j = 0$, $\gamma = 1.3$, $y = 0$).

nondimensional static and dynamic pressure* impulses

$$I_1(\tau) = \int_1^{\tau} \frac{p}{p_n} d\tau \quad (32)$$

$$I_2(\tau) = \int_1^{\tau} \frac{q}{q_n} d\tau \quad (33)$$

as a function of time τ. At the end of the "positive phase" ($\tau = 2$), the integrals reach the following values for the case of $\gamma = 1.3$: $I_1(\tau = 2) = 0.5513$ and $I_2(\tau = 2) = 0.1818$. This figure can be used to evaluate the overpressure and dynamic pressure partial impulses from the following relations:

$$I_{\Delta p}(t/t_n) = \int_{t_n}^{t} \Delta p dt$$

$$= p_n t_n I_1(\tau) - p_a t_n(\tau-1) \quad (34)$$

$$I_q(t/t_n) = \int_{t_n}^{t} q dt$$

$$= q_n t_n I_2(\tau) \quad (35)$$

*Dynamic pressure defined as $q = \frac{1}{2}\rho u^2$.

III. APPLICATIONS

1. PROPERTIES OF DETONATABLE GASES

Table 1a shows the detonation properties of gaseous mixtures as originally calculated and measured by Jouguet (1905-6). With improved thermochemical data, Lewis and von Elbe (1961) calculated the detonation properties for hydrogen-oxygen systems given in Table 1b. Table 1c presents detonation velocities for hydro-carbon plus oxygen or air mixtures from Shchelkin and Troshin (1965). Detonation velocities for hydrogen-oxygen systems range from 1.7 to 3.5 km/s depending on the mixture, while detonation pressures vary from p_n = 14 to 18 atm; detonation temperatures range from 2600 to 3600 K. Acetylene (C_2H_2) or cyanogen (C_2N_2) plus oxygen mixtures have considerably higher detonation pressures (∿55 bars) and temperatures approaching 6000 K.

2. SIMULATION FIDELITY

As a representative case, we consider here a stoichiometric mixture of hydrogen and oxygen ($H_2+\frac{1}{2}O_2$) at atmospheric pressure and temperature. The detonation jump conditions are listed in Table 2. Detonation pressure is 17.6 atm, while the peak dynamic pressure and temperature are 6 atm and about 3660 K, respectively.

Figure 5 compares the time histories for a planar, CJ detonation wave solution ($j = 0$, $\gamma = 1.3$, $y = 0$) with a nuclear surface burst explosion for the case where the peak pressures have been matched at p_n = 17.6 atm (Δp_n = 244 psi). Times have been scaled by the wave arrival time at the station of interest. Notice that the CJ pressure waveform decays much more slowly than the nuclear case. This is very

TABLE 1. PROPERTIES OF DETONATION WAVES IN GASEOUS MIXTURES AT 1 ATM PRESSURE

Gas mixture	T_1 (°K)	T_2	$\frac{p_2}{p_1}$	$\frac{\rho_2}{\rho_1}$	Velocity (m/s)	Velocity observed (m/s)
$H_2 + O$	10	3956	1.879	17.5	2629	2810 / 2821
$H_2 + O$	100	3681	1.864	12.9	2815	2790
$H_2 + O + 5H$	10	2586	1.79	14.4	3526	3530
$H_2 + O + 5N$	10	2586	1.79	14.4	1798	1822
$H_2 + O + 5O$	10	2586	1.79	14.4	1682	1707
$CO + O$ + humidity	10	3862	1.887	17.2	1864	1676
$CO + O$ + humidity	35	3748	1.88	15.6	1860	1738
$CO + H_2 + O_2$	10	3800	1.881	17.3	1894	2008 / 2143
$C_2H_2 + 3O_2$	10	4080	1.91	28.8	2120	2220
$C_2H_2 + 10O_2$	10	3680	1.84	22.0	1868	1860
$C_2H_2 + O_2$	10	5670	1.84	54.5	3091	2961
$C_2N_2 + O_2$	10	5980	1.837	58.2	2646	2728
$C_2N_2 + O_2 + 2N_2$	10	4344	1.8	33.7	2214	2166
$CH_4 + O_2$	10	3060	1.836	28.8	2477	2528
$C_2H_4 + 3O_2$	10	6160	1.914	34.8	2075	2196 / 2321
$CH_4 + 2O_2$	10	4080	1.904	27.4	2220	2287 / 2322
$CH_4 + 4O_2$	10	3670	1.88	22.4	2130	2166
$H + Cl$	10	3880	1.787	24.8	1861	1729
$H + Cl + H_2$	10	3400	1.73	14.7	2000	1866
$N_2O + H_2$	10	3833	1.886	26.8	2360	2284 / 2306

1a. Calculated and measured by Jouguet (1905 - 06)

Explosive mixture	p_2 (atm)	T_2 (°K)	Detonation velocity (m/s)		Concentration (% of burned gas)	
			Calc	Expt	OH	H
$(2H_2 + O_2)$	18.05	3583	2806	2819	26.3	6.9
$(2H_2 + O_2) + 1O_2$	17.4	3390	2302	2314	38.6	1.8
$(2H_2 + O_2) + 3O_2$	15.3	2970	1925	1922	13.5	0.2
$(2H_2 + O_2) + 5O_2$	14.13	2620	1730	1700	8.3	0.07
$(2H_2 + O_2) + 1N_2$	17.37	3367	2378	2407	14.2	3.3
$(2H_2 + O_2) + 3N_2$	15.63	3062	2033	2055	5.9	0.9
$(2H_2 + O_2) + 5N_2$	14.39	2685	1850	1822	2.1	0.2
$(2H_2 + O_2) + 2H_2$	17.25	3314	3354	3273	5.9	6.5
$(2H_2 + O_2) + 4H_2$	15.97	2976	3627	3527	1.2	3.0
$(2H_2 + O_2) + 6H_2$	14.19	2650	3749	3532	0.3	1.1

$T_1 = 291°K$

1b. Calculated and measured by Lewis and Von Elbe (1961)

Mixture	Velocity of detonation (m/s)
$2H_2 + O_2$	2821
$2CO + O_2$ (+5.6% H_2O)	1,766
$CS_2 + 3O_2$	1,800
$CH_4 + 2O_2$	2,320
$C_2H_2 + 2.5O_2$	2,363
$C_3H_8 + 5O_2$	2,600
$C_5H_{12} + 8O_2$	2,371
$C_6H_6 + 7.5O_2$	2,300
H_2 + air stoichiometric mixture	1,800
C_5H_{12} + air stoichiometric mixture	1,710
C_6H_6 + air stoichiometric mixture	1,610
Ethyl ether + air (4.3% ether)	1,762

$T_0 = 293°K$.

1c. From Shchelkin and Troshin (1965)

TABLE 2. DETONATION CONDITIONS FOR A STOICHIOMETRIC H_2-O_2 MIXTURE (w_n = 2.821 km/s)

	Detonation		Air shock
	Ambient	State n	
p (atm)	1.0	17.6	17.6
ρ (g/cm^3)	0.503×10^{-3}	0.867×10^{-3}	5.74×10^{-3}
T (°K)	291	~ 3660	291
M (g/g mole)	12	~ 15	29
γ	1.4	~ 1.30	1.37
a (km/s)	0.531	1.624	0.646
u (km/s)	0	1.813	1.04
q (atm)	0	6.067	31.0
w_n (km/s)	-	2.82	1.32

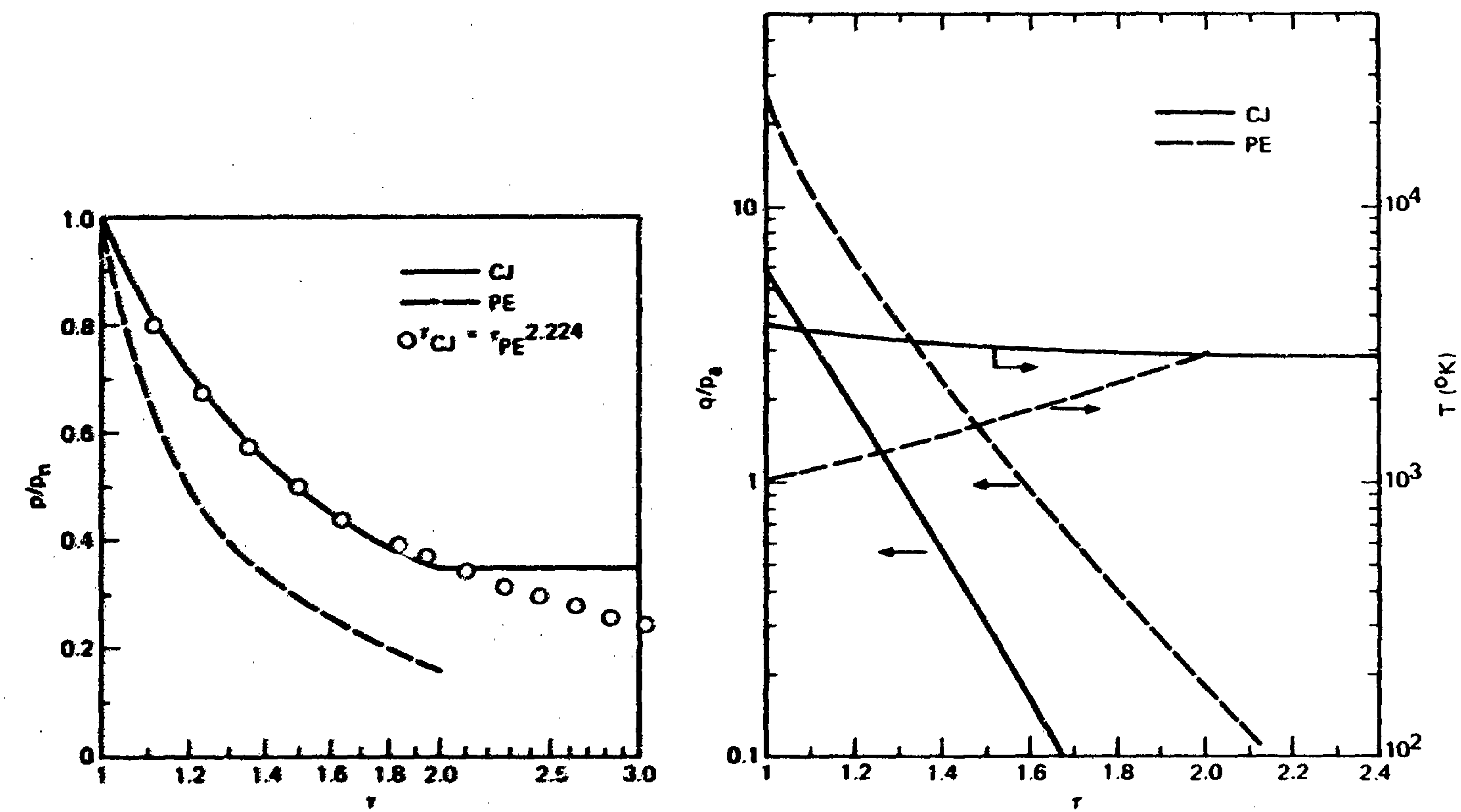

Figure 5. Comparison of the time histories for the planar Chapman-Jouguet detonation wave solution (CJ) and a nuclear surface burst explosion (PE) for the case of matched peak pressures ($p_n \approx 17.6$ atm).

advantageous because it will reduce the required tube length for the simulator. The time scale for the nuclear case can be stretched to fit the CJ solution according to the relation:

$$\tau_{CJ} = \tau_{PE}{}^{2.224} \tag{36}$$

which is denoted by the circled points on Figure 5. Hence, to good approximation, one finds:

$$p/p_n = [(0.3/\tau_{CJ}+1)/1.3]^{26/3}$$

$$= [(0.3/\tau_{PE}{}^{2.224}+1)/1.3]^{26/3} \tag{37}$$

It is clear from the above comparisons that the detonation tube simulator does a good job at replicating the pressure waveforms of a nuclear surface burst for times $1 \leq \tau_{CJ} \leq 2$. The next question is: how well does it match the other environments? Figure 5 compares the dynamic pressure histories for the CJ and PE cases. The waveforms have the same shape; however, the air shock has a much higher peak dynamic pressure (31 atm) than the CJ detonation (6 atm). This is caused principally by the low initial density of the H_2-O_2 mixture at ambient pressure and temperature (which is, in turn, related to its smaller molecular weight of 12 versus 29 for air). This peak dynamic pressure can be increased by choosing reactants with large molecular weights. One of the best mixtures in this regard is a cyanogen-oxygen mixture ($C_2N_2+2O_2$) which gives a peak dynamic pressure of 34.6 atm.

There are significant differences in the temperature histories for the CJ and PE cases, as demonstrated in Figure 5. At the 17.6-atm station, the air is shock-heated to a temperature of about 1000 K and increases to about 3000 K during the simulation time ($1 \leq \tau \leq 2$), while the CJ temperature history starts at the detonation temperature (~3700 K for the H_2-O_2 system considered) and decays to about 3000 K at $\tau = 2$. At these gas temperatures small dust particles can melt and/or vaporize due to convective heat transfer between the detonation products and the dust (e.g., SiO_2 has a melt temperature of 1900 K and a vaporization temperature of 2500 K). Although air temperatures are too small to cause this effect in the nuclear case (until a time of τ = 1.6 to 1.8), the dust particles will be heated by the nuclear fireball radiation, and may melt and/or vaporize due to radiative heat transfer. To resolve this issue, detailed heat transfer calculations should be performed for dust particles of interest. It will probably be difficult to find gaseous mixtures with comoustion temperatures much below 2500 K, so if heat transfer is a problem, then it will place limits on the range of applicability of the simulator. Alternatively, one could match the detonation temperature; a 3500 K air shock temperature corresponds to a shock overpressure of about 100 atm.

Current theories of boundary layer scouring of dust from surfaces attempt to relate mass injection rates to the wall shear stress. This is, in turn, related to the dynamic pressure just outside the boundary layer. Hence, the dynamic pressure appears to be the most important flow parameter. Figure 6 compares the dynamic pressure time histories for the detonation tube simulator (using the H_2+O_2 system shown in Figure 5) with those of the PE case at matched peak dynamic pressures (q_n = 6 atm). It is clear from Figure 6 that the CJ waveform is a good approximation to the PE waveform over most of the positive phase; hence, for scaling purposes

$$\tau_{CJ} = \tau_{PE} \tag{38}$$

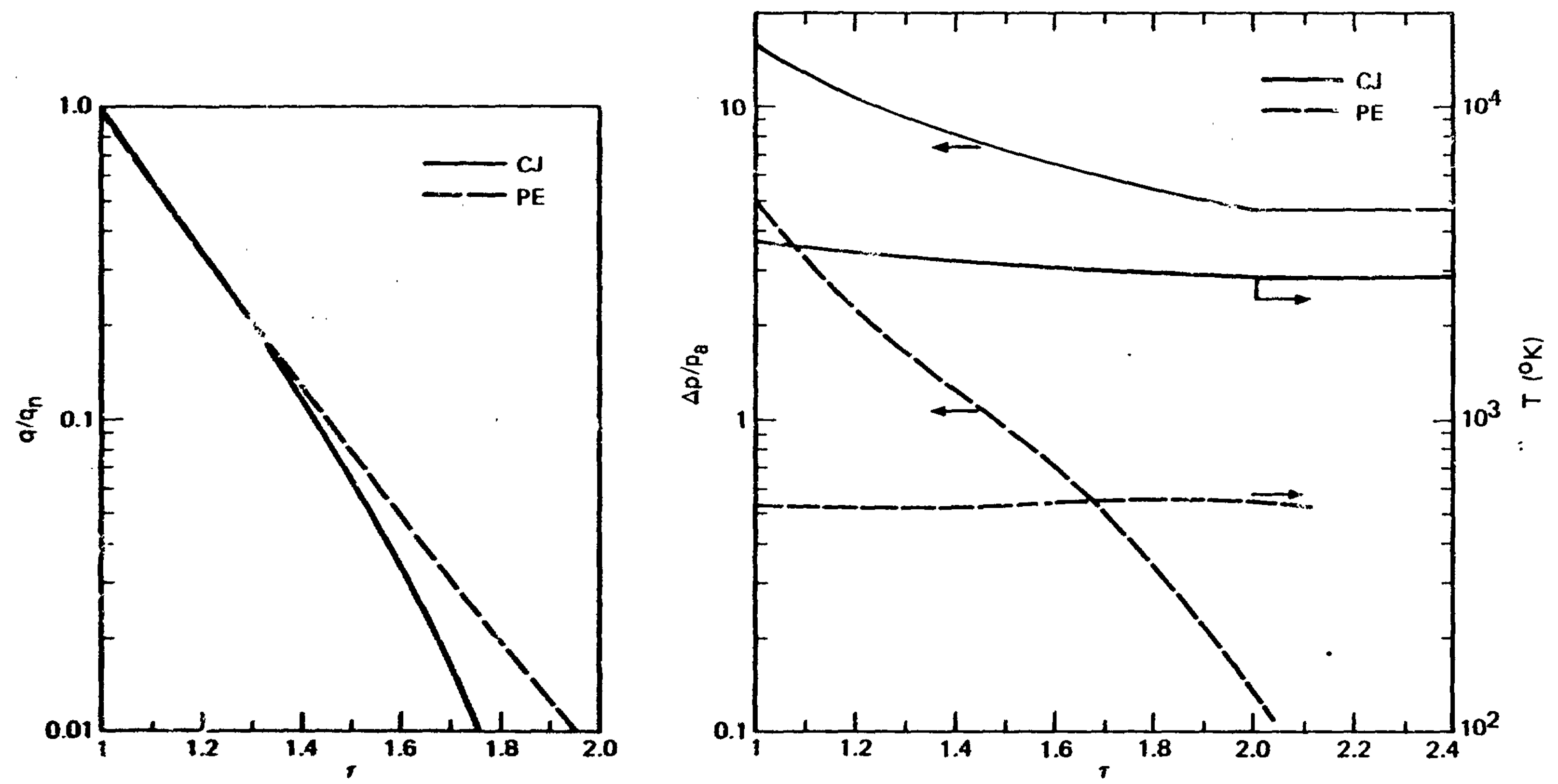

Figure 6. Comparison of the time histories for the planar Chapman-Jouguet detonation wave solution (CJ) and a nuclear point explosion (PE) for the case of matched peak dynamic pressures ($q_n \approx 6$ atm).

for dynamic pressures. The analytic form for the dynamic pressure history then becomes

$$q/q_n = (2/\tau-1)^2[(0.3/\tau+1)/1.3]^{20/3}. \quad (39)$$

In this case the peak overpressures are no longer matched (Δp_n = 16.6 atm in the CJ case, and $\Delta p_n \sim 5$ atm in the PE case). Temperatures are also mismatched, as before.

3. SCALING

Next let us consider scaling relations for the detonation tube blast wave simulator. We start by equating simulation times:

$$\Delta t_{CJ} = \Delta t_{PE} \quad (40)$$

or

$$t_{n_{CJ}}(\tau_{CJ}-1) = t_{n_{PE}}(\tau_{PE}-1). \quad (41)$$

Solving for $t_{n_{CJ}}$ and noting that $\tau_{CJ} = \tau_{PE}^{\alpha}$ (where α = 2.224 for static pressure wave forms and α = 1 for dynamic pressure wave forms according to Equations (36) and (38), respectively), one finds

$$t_{n_{CJ}} = t_{n_{KT}} W^{1/3}(\tau_{PE}-1)/(\tau_{PE}^{\alpha}-1) \quad (42)$$

where $t_{n_{KT}}$ = shock arrival time in ms/$KT_{SB}^{1/3}$, and

W = equivalent nuclear burst yield in kilotons.

The above relation can be used to determine the detonation run length ($L = W_{CJ}t_{n_{CJ}}$) needed to provide the required simulation time:

$$L = W_{CJ}t_{nKT}\ W^{1/3}(\tau_{PE}-1)/(\tau_{PE}^{\alpha}-1). \qquad (43)$$

This distance is considered to be the appropriate location of the dusty flow measure devices. As shown in Table 3, a run length of 26 $m/KT_{SB}^{1/3}$ is required to simulate the pressure wave form at the p_n = 17.6 atm (Δp = 244 psig) station for a kiloton surface burst with a stoichiometric mixture of hydrogen and oxygen. With this same mixture, a run length of 182 $m/KT_{SB}^{1/3}$ is required to simulate a kiloton dynamic pressure wave form at the q_n = 6 atm (88 psi) station. As one goes to smaller pressures, the nuclear waveforms broaden; hence, longer run lengths are required. To achieve larger dynamic pressures one can use, for example, an acetylene-oxygen mixture ($C_2H_2+O_2$) with a peak dynamic pressure of 18 atm and a run length of 105 $m/KT_{SB}^{1/3}$, or a cyanogen-oxygen mixture ($C_2N_2+2O_2$) with a peak dynamic pressure of 35 atm and a run length of 66 $m/KT_{SB}^{1/3}$.

4. DESIGN CONSIDERATIONS

Next we offer the following practical considerations for fielding a blast wave simulator: the choce of gaseous mixture, a technique for filling the detonation tube, and approaches to minimize the tube length (hence, minimize cost). The current costs of a few candidate gases are:

H_2 gas: \$5 per 100 ft^3 (at 2000 psi and 291 K)
O_2 gas: \$1.87 per 100 ft^3 (at 2000 psi and 291 K)
C_2H_2 gas: \$14.75 per 100 ft^3 (at 250 psi and 291 K)
C_2N_2 gas: \$340 per lb (2-in dia x 13-in cylinder)

TABLE 3. REQUIRED DETONATION RUN LENGTHS

	Simulator			
	p-waveform (p_n = 17.6 atm)	q-waveform (q_n = 6 atm)	q-waveform (q_n = 18 atm)	q-waveform (q_n = 34 atm)
t_{nPE} (ms/$KT_{SB}^{1/3}$)	25.4	64.6	35.4	24.2
Δt^* (ms/$KT_{SB}^{1/3}$)	9.27	64.6	35.4	24.2
τ_{PE}^*	1.365	2.0	2.0	2.0
τ_{CJ}^*	2.0	2.0	2.0	2.0
α	2.224	1	1	1
Gas mixture	$2H_2 + O_2$	$2H_2 + O_2$	$C_2H_2 + O_2$	$C_2N_2 + 2O_2$
w_{nCJ} (km/s)	2.821	2.821	2.961	2.728
L (m/$KT_{SB}^{1/3}$)	26	182	105	66

*Denotes simulation duration

Cyanogen (C_2N_2) appears to be prohibitively expensive. Assuming a 1-m^2 tube cross section, it would cost about $5 to fill a 115-m-long tube with acetylene for an 18-atm dynamic pressure simulator, and less than $1 to fill a 35-m-long tube with $2H_2+O_2$ as an 18-atm static pressure simulator. Clearly these are negligible costs.

Perhaps the simplest way of filling the tube with a detonable gas mixture is to use air as the oxidizer and slowly bleed in the fuel gas. Utilizing air instead of O_2 gas will reduce the detonation velocity to about 1.9 km/s (which will reduce the run length required by about 30 percent) and reduce the detonation temperature to perhaps 2700 K--both of which are beneficial effects. Also, one would like to choose a gas mixture which has a high molecular weight, to achieve large peak dynamic pressures. Taking all these factors into consideration, it appears that a stoichiometric mixture of acetylene and air is one of the best choices for the detonatable gas. It is inexpensive ($\sim$\$5 per 100-m^3 test), it gives large peak dynamic pressures, and it is readily available.

Probably the largest expense item of the simulator is the construction cost of building the tube. This, in turn, is related to the tube length. Simulation time requirements fix the detonation run length, but a downstream tube section is also required. This end of the tube could be sealed with a thin plastic sheet, and terminated with a survivable louvered end section (Crosnier et al., 1974) to eliminate rarefactions from this "semi-open" end and minimize the tube length.

IV. CONCLUSIONS

When a planar detonation wave is initiated at the closed end of a tube, it induces a peaked blast wave which expands self-similarly with time. Being forced by the physics, this happens naturally. The preceding analysis demonstrated that the static and dynamic pressure waveforms associated with a planar CJ detonation give a high-fidelity simulation of either the static or dynamic pressure environment (but not both at the same time) of a nuclear surface burst for times $1 \leq \tau_{CJ} \leq 2$. One can achieve peak overpressures from 14 to 55 atm and peak dynamic pressures from 6 to 35 atm, depending upon the detonatable gas selected. This phenomenon could be utilized in a disposable detonation tube to impose peaked blast waves on in-situ ground surfaces of interest, and then measure the properties of the ensuing dusty (or clean) blast wave boundary layer. Detonation tube lengths from 25 to 100 $m/KT_{SB}^{1/3}$ are required to simulate yields in the kiloton range.

The principal deficiency of this technique is that the detonation products have temperatures (~3000 K) which are significantly larger than their airblast counterparts (~1000 K). Small (10-μm diameter) dust particles have the potential for melting and vaporizing due to convective heat transfer. These effects can be ameliorated somewhat by choosing air as the oxidizer and by using large diameter dust particles.

REFERENCES

1. Chapman, D., Phil. Mag. 47, 1899, p. 90.

2. Courant, R., and Friedrichs, K. O., Supersonic Flow and Shock Waves, Interscience, 1948.

3. Crosnier, J. R., et al., "Concepts and Design for a Large Diameter, High Performance Blast Simulator," Fourth Int. Symposium on the Military Application of Blast Simulation, 9-12 September 1974, Southend-on-Sea, England.

4. Gilette, D. A., et al., "Threshold Friction Velocities and Rupture Moduli for Crusted Desert Soils for Input of Soil Particles into the Air," J. Geophysical Research, Vol. 87, C11, 1982, 9003-9015.

5. Jouguet, M., J. Math (6) 1, 1905-6, p. 347.

6. Kuhl, A. L., and Seizew, M. R., Analysis of Ideal, Strong Chapman-Jouguet Detonations, TRW Report 7814735.9-13, TRW, Redondo Beach, CA, 1978.

7. Lewis B., and Von Elbe, G., Combustion, Flames and Explosions of Gases, 2nd Edition, Academic Press Inc., New York, NY, 1961.

8. Oppenheim, A. K., Kuhl, A. L., and Kamel, M. M., "On Self-Similar Blast Waves Headed by the Chapman-Jouguet Detonation," J. Fluid Mech., 55, Part 2, 1972, pp. 257-270.

9. Renick, J. D., "Some Considerations in the Design of a Dynamic Airblast Simulator," Sixth Symposium (Int.) on the Military Applications of Blast Simulations, 25-29 June 1974, Cahors, France.

10. Shchlelkin, K. J., and Troshin, Ya. K., Gasdynamics of Combustion, Translated by B. W. Kuvshinoff and L. Holtschlag, Mono Book Corp., Baltimore, MD, 1965.

11. Stanyukovich, K. P., Unsteady Motion of Continuous Media, Moscow, Gostokhizdat, Translated 1960, ed. M. Holt, Pergamon Press, New York, NY, 1959.

12. Taylor, G. I., "The Dynamics of the Combustion Products Behind Plane and Spherical Detonation Fronts in Explosives," Proc. Royal Soc. A 200, 1950, pp. 235-247.

DISTRIBUTION LIST

DEPARTMENT OF DEFENSE

Defense Intelligence Agency
ATTN: RTS-2A

Defense Nuclear Agency
ATTN: SPSS, G. Ullrich
ATTN: SPSS, T. Deevy
4 cy ATTN: TITL

Defense Tech Info Ctr
12 cy ATTN: DD

Field Command
Defense Nuclear Agency
ATTN: FCTT
ATTN: FCPR
ATTN: FCTXE
ATTN: FCTT, G. Ganong
ATTN: FCTT, W. Summa

Joint Strat Tgt Planning Staff
ATTN: XPFS

Under Secretary of Defense for Rsch & Engrg
ATTN: Strategic & Space Sys (OS)
ATTN: Strat & Theater Nuc Forces, B. Stephan

DEPARTMENT OF THE ARMY

BMD Advanced Technology Ctr
ATTN: ATC-T

BMD Systems Command
ATTN: BMDSC-HLE, R. Webb

Chief of Engineers
ATTN: DAEN-MPE-T

Harry Diamond Labs
ATTN: DELHD-NW-P
ATTN: DELHD-TA-L

US Army Ballistic Rsch Labs
ATTN: DRDAR-BLA-S
ATTN: DRDAR-BLT, J. Keefer

US Army Engineer Ctr & Ft Belvoir
ATTN: Tech Library

US Army Engineer Div, Huntsville
ATTN: HNDED-FD

US Army Nuclear & Chemical Agency
ATTN: Library
ATTN: MONA-WE, J. Uecke

DEPARTMENT OF THE NAVY

Naval Research Lab
ATTN: Code 2627
ATTN: Code 4040, J. Boris
ATTN: Code 4040, D. Book

Naval Surface Weapons Ctr
ATTN: Tech Library & Info Svcs Br

DEPARTMENT OF THE NAVY (Continued)

Naval Surface Weapons Ctr
ATTN: Code F31
ATTN: Code X211
ATTN: R44, H. Glaz

DEPARTMENT OF THE AIR FORCE

Air Force Institute of Technology
ATTN: Library

Air Force Weapons Lab
ATTN: SUL
ATTN: NT, D. Payton
ATTN: NTED-A

Assistant Chief of Staff
Studies & Analyses
ATTN: AF/SAMI, Tech Info Div

Ballistic Missile Office
ATTN: EN, C. Case
ATTN: ENSN, A. Schenker
ATTN: ENBF, D. Gage

Strategic Air Command
ATTN: XPFS, Maj Skluzacek
ATTN: INT, E. Jacobsen
ATTN: NRI-STINFO, Library

OTHER GOVERNMENT AGENCY

Central Intelligence Agency
ATTN: OSWR/NED

FOREIGN AGENCIES

Defence Research Establishment, Suffield
ATTN: Dr J. Moen

University of Toronto
ATTN: Prof I. Glass

DEPARTMENT OF ENERGY CONTRACTORS

Los Alamos National Lab
ATTN: R. Sanford
ATTN: C. Keller

Sandia National Lab
ATTN: Div 1111, J. Reed
ATTN: Org 7112, A. Chabai
ATTN: J. Banister

DEPARTMENT OF DEFENSE CONTRACTORS

Acurex Corp
ATTN: C. Wolf

Aerospace Corp
ATTN: H. Mirels
ATTN: Tech Info Svcs

Applied Research Assoc, Inc
ATTN: D. Piepenburg

DEPARTMENT OF DEFENSE CONTRACTORS (Continued)

Applied Research Assoc, Inc
ATTN: J. Bratton
ATTN: N. Higgins

Applied Theory, Inc
2 cy ATTN: J. Trulio

Boeing Co
ATTN: Aerospace Library
ATTN: S. Strack

California Rsch & Technology, Inc
ATTN: K. Kreyenhagen
ATTN: Library

University of Denver
ATTN: Sec Officer for J. Wisotski

H-Tech Labs, Inc
ATTN: B. Hartenbaum

J. D. Haltiwanger Consulting Svcs
ATTN: W. Hall
ATTN: J. Haltiwanger

Kaman AviDyne
ATTN: R. Ruetenik

Kaman Sciences Corp
ATTN: D. Sachs

Kaman Tempo
ATTN: DASIAC

McDonnell Douglas Corp
ATTN: D. Dean
ATTN: H. Herdman
ATTN: R. Halprin

Mission Research Corp
ATTN: C. Longmire

University of New Mexico
ATTN: P. Lodde
ATTN: CERF, G. Leigh
ATTN: J. Kovarna

Pacific-Sierra Rsch Corp
ATTN: H. Brode, Chairman SAGE

Pacific-Sierra Rsch Corp
ATTN: D. Gormley

Pacifica Technology
ATTN: R. Allen
ATTN: Tech Library

Patel Enterprises, Inc
ATTN: M. Patel

DEPARTMENT OF DEFENSE CONTRACTORS (Contractors)

Physical Research, Inc
ATTN: R. Deliberis

Physics International Co
ATTN: F. Sauer
ATTN: Tech Library
ATTN: J. Thomsen

R & D Associates
ATTN: Tech Info Ctr
ATTN: J. Carpenter
ATTN: P. Haas
4 cy ATTN: A. Kuhl

S-CUBED
ATTN: Library
ATTN: C. Dismukes
ATTN: K. Pyatt
ATTN: J. Barthel

S-CUBED
ATTN: C. Needham

Science & Engrg Assoc, Inc
ATTN: B. Chambers, III

Science Applications, Inc
ATTN: Tech Library
ATTN: R. Schlaug
ATTN: H. Wilson

Science Applications, Inc
ATTN: G. Binniger
ATTN: W. Layson
ATTN: J. Cockayne

SRI International
ATTN: Library
ATTN: J. Colton
ATTN: G. Abrahamson

Teledyne Brown Engrg
ATTN: D. Ormond
ATTN: J. McSwain
ATTN: F. Leopard
ATTN: J. Ford

TRW Electronics & Defense Sector
ATTN: T. Mazzola
ATTN: N. Lipner
ATTN: Tech Info Ctr

TRW Electronics & Defense Sector
ATTN: P. Dai
ATTN: E. Wong
ATTN: G. Hulcher

Weidlinger Assoc, Consulting Engrg
ATTN: I. Sandler